

Seasonal Dynamics of Epiphytic Microbial Communities on Marine Macrophyte Surfaces

1†

† To whom correspondence should be addressed: marino.korlevic@irb.hr

1. Ruđer Bošković Institute, Center for Marine Research, G. Paliaga 5, Rovinj, Croatia
2. University of Vienna, Department of Limnology and Bio-Oceanography, Althanstraße 14, Vienna, Austria

1 **Abstract**

2 Introduction

3 Marine macrophytes (seagrasses and macroalgae) are important ecosystem engineers that
4 form close associations with microorganism belonging to all three domains of life (Egan *et al.*,
5 2013; Tarquinio *et al.*, 2019). Microbes can live within macrophyte tissue as endophytes or can
6 form epiphytic communities on surfaces of leaves and thalli (Egan *et al.*, 2013; Hollants *et al.*,
7 2013; Tarquinio *et al.*, 2019). Epiphytic and endophytic microbial communities form a close
8 functional relationship with the macrophyte host. It was proposed that this close relationship
9 constitutes a holobiont, an integrated community where the macrophyte organism and its symbiotic
10 partners support each other (Margulis, 1991; Egan *et al.*, 2013; Tarquinio *et al.*, 2019).

11 Biofilms formed from microbial epiphytes can contain diverse taxonomic groups and harbor
12 cell densities from 10^2 to 10^7 cells cm^{-2} (Armstrong *et al.*, 2000; Bengtsson *et al.*, 2010; Burke *et*
13 *al.*, 2011b). In such an environment a number of positive and negative interactions between the
14 macrophyte and colonizing microorganisms have been described (Egan *et al.*, 2013; Hollants *et*
15 *al.*, 2013; Tarquinio *et al.*, 2019). Macrophytes can promote growth of associated microbes by
16 nutrient exudation, while in return microorganisms may support macrophyte performance through
17 improved nutrient availability, phytohormone production and protection form toxic compounds,
18 oxidative stress, biofouling organisms and pathogens (Egan *et al.*, 2013; Hollants *et al.*, 2013;
19 Tarquinio *et al.*, 2019). Beside this positive interactions, macrophytes can negatively impact
20 the associated microbes such as pathogenic bacteria by producing reactive oxygen species and
21 secondary metabolites (Egan *et al.*, 2013; Hollants *et al.*, 2013; Tarquinio *et al.*, 2019).

22 All these ecological roles are carried out by a taxonomically diverse community of
23 microorganisms. At higher taxonomic ranks a core set of macrophyte epiphytic taxa was
24 described consisting mainly of *Alphaproteobacteria*, *Gammaproteobacteria*, *Desulfobacterota*,
25 *Bacteroidota*, *Cyanobacteria*, *Actinobacteriota*, *Firmicutes*, *Planctomycetota*, *Chloroflexi* and
26 *Verrucomicrobiota* (Crump and Koch, 2008; Tujula *et al.*, 2010; Lachnit *et al.*, 2011). In contrast,

27 at lower taxonomic ranks host specific microbial communities were described (Lachnit *et al.*,
28 2011; Roth-Schulze *et al.*, 2016). Recently, it was shown that even different morphological niches
29 within the same alga had a higher influence on bacterial community variation than biogeography
30 or environmental factors (Morrissey *et al.*, 2019). While there is high community variation
31 between host species is was observed that the majority of metagenome determined functions were
32 conserved both between host species and individuals (Burke *et al.*, 2011a; Roth-Schulze *et al.*,
33 2016). This discrepancy between taxonomic and functional composition could be explained by
34 the lottery hypothesis. It postulates that an initial random colonization step is performed from
35 a set of functionally equivalent taxonomic groups resulting in taxonomically different epiphytic
36 communities sharing a core set of functional genes (Burke *et al.*, 2011a; Roth-Schulze *et al.*,
37 2016). In addition, some of the variation in the observed data could be attributed to different
38 techniques used in various studies, such as different protocols for epiphytic cell detachment and/or
39 DNA isolation, as no standard protocol to study epiphytic communities was established (Ugarelli
40 *et al.*, 2019; Korlević *et al.*, submitted).

41 The majority of studies describing macrophyte epiphytic communities did not encompass
42 seasonal changes (Crump and Koch, 2008; Lachnit *et al.*, 2009; Burke *et al.*, 2011b; Roth-Schulze
43 *et al.*, 2016; Ugarelli *et al.*, 2019). In addition, if seasonal changes were taken into account
44 low temporal frequency and/or methodologies that do not allow for high taxonomic resolution
45 were used (Tujula *et al.*, 2010; Lachnit *et al.*, 2011; Miranda *et al.*, 2013). In the present study
46 we describe the seasonal dynamics of bacterial and archaeal communities on the surfaces of
47 the seagrass *Cymodocea nodosa* and siphonous macroalgae *Caulerpa cylindracea* determined
48 on a mostly monthly scale. Bacterial and archaeal epiphytes were sampled in a meadow of
49 *Cymodocea nodosa* invaded by the invasive *Caulerpa cylindracea* and in a locality of only
50 *Caulerpa cylindracea* located in the proximity of the meadow. In addition, for comparison, the
51 community of the surrounding seawater was characterized.

52 **Materials and Methods**

53 **Sampling**

54 Leaves of *Cymodocea nodosa* were sampled in a *Cymodocea nodosa* meadow located in the
55 proximity of the village of Funtana (45°10'39" N, 13°35'42" E). Thalli of *Caulerpa cylindracea*
56 were sampled in the same *Cymodocea nodosa* invaded meadow in Funtana and on a locality of
57 only *Caulerpa cylindracea* located close to the invaded meadow. Sampling of leaves and thalli
58 was performed approximately monthly from December 2017 to October 2018 (Table S1). Leaves
59 and thalli were collected by diving and transported to the laboratory in containers placed on ice
60 and filled with site seawater. Upon arrival to the laboratory, *Cymodocea nodosa* leaves were cut
61 into sections of 1 – 2 cm, while *Caulerpa cylindracea* thalli were cut into 5 – 8 cm long sections.
62 Leaves and thalli were washed three times with sterile artificial seawater (ASW) to remove loosely
63 attached microbial cells. Surrounding seawater was collected in 10 l containers by diving and
64 transported to the laboratory where the whole container volume was filtered through a 20 µm net.
65 The filtrate was further sequentially filtered through 3 µm and 0.2 µm polycarbonate membrane
66 filters (Whatman, United Kingdom) using a peristaltic pump. Filters were briefly dried at room
67 temperature and stored at –80 °C. Seawater samples were also collected approximately monthly
68 from July 2017 to October 2018.

69 **DNA Isolation**

70 DNA from surfaces of *Cymodocea nodosa* and *Caulerpa cylindracea* was isolated using
71 a previously modified and adapted protocol that allows for a selective epiphytic DNA isolation
72 (Massana *et al.*, 1997; Korlević *et al.*, submitted). Briefly, leaves and thalli are incubated
73 in a lysis buffer and treated with lysozyme and proteinase K. Following the incubations, the
74 mixture containing lysed epiphytic cells is separated from leaves and thalli and extracted using

75 a phenol-chloroform procedure. Finally, the extracted DNA is precipitated using isopropanol.
76 DNA from seawater picoplankton was isolated from 0.2 µm polycarbonate filters according to
77 (Massana *et al.*, 1997) with a slight modification. Following the phenol-chloroform extraction
78 steps 1/10 of chilled 3 M sodium acetate (pH 5.2) was added. DNA was precipitated by adding
79 1 volume of chilled isopropanol, incubating the mixtures overnight at –20 °C and centrifuging at
80 20,000 × g and 4 °C for 21 min. The pellet was washed twice with 500 µl of chilled 70 % ethanol
81 and centrifuged after each washing step at 20,000 × g and 4 °C for 5 min. Dried pellets were
82 resuspended in 50 – 100 µl of deionized water.

83 **Illumina 16S rRNA Sequencing**

84 Illumina MiSeq sequencing of the V4 16S rRNA region was performed as described
85 previously (Korlević *et al.*, submitted). The V4 region of the 16S rRNA gene was amplified using
86 a two-step PCR procedure. In the first PCR the 515F (5'-GTGYCAGCMGCCGCGTAA-3')
87 and 806R (5'-GGACTACNVGGGTWTCTAAT-3') primers from the Earth Microbiome Project
88 (<http://press.igsb.anl.gov/earthmicrobiome/protocols-and-standards/16s/>) were used (Caporaso
89 *et al.*, 2012; Apprill *et al.*, 2015; Parada *et al.*, 2016). These primers contained on their 5' end
90 a tagged sequence. Purified PCR products were sent for Illumina MiSeq sequencing at IMGM
91 Laboratories, Martinsried, Germany. Before sequencing at IMGM, the second PCR amplification
92 of the two-step PCR procedure was performed using primers targeting the tagged region
93 incorporated in the first PCR. In addition, these primers contained adapter and sample-specific
94 index sequences. Beside samples, a positive and negative control for each sequencing batch was
95 sequenced. Negative control was comprised of PCR reactions without DNA template, while for a
96 positive control a mock community composed of evenly mixed DNA material originating from 20
97 bacterial strains (ATCC MSA-1002, ATCC, USA) was used. The sequences obtained in this study
98 have been submitted to the European Nucleotide Archive (ENA) under accession numbers **TO BE**

99 **ADDED LATER!**

100 **Sequence Analysis**

101 Obtained sequences were analyzed on the computer cluster Isabella (University Computing
102 Center, University of Zagreb) using mothur (version 1.43.0) (Schloss *et al.*, 2009) according
103 to the MiSeq Standard Operating Procedure (MiSeq SOP; https://mothur.org/wiki/MiSeq_SOP)
104 (Kozich *et al.*, 2013) and recommendations given from the Riffomonas project to enhance data
105 reproducibility (<http://www.riffomonas.org/>). For alignment and classification of sequences
106 the SILVA SSU Ref NR 99 database (release 138; <http://www.arb-silva.de>) was used (Quast *et*
107 *al.*, 2013; Yilmaz *et al.*, 2014). Pipeline data processing and visualization was done using R
108 (version 3.6.0) (R Core Team, 2019), packages vegan (version 2.5-6) (Oksanen *et al.*, 2019), and
109 tidyverse (version 1.3.0) (Wickham *et al.*, 2019) and multiple other packages (Xie, 2014, 2015,
110 2019a, 2019b, 2020; Neuwirth, 2014; Xie *et al.*, 2018; Allaire *et al.*, 2019; Zhu, 2019). The
111 detailed analysis procedure including the R Markdown file for this paper are available as a GitHub
112 repository (**TO BE ADDED LATER!**). Based on the ATCC MSA-1002 mock community
113 included in the analysis an average sequencing error rate of 0.01 % was determined, which is in
114 line with previously reported values for next-generation sequencing data (Kozich *et al.*, 2013;
115 Schloss *et al.*, 2016). In addition, the negative controls processed together with the samples
116 yielded on average only 2 sequences after sequence quality curation.

117 **Results**

118 Sequencing of the 16S rRNA V4 region yielded a total of 1.8 million sequences after
119 quality curation and exclusion of eukaryotic, chloroplast, mitochondrial and no relative sequences
120 (Table S1). A total of 35 samples originating from epiphytic archaeal and bacterial communities
121 associated with surfaces of the seagrass *Cymodocea nodosa* and macroalga *Caulerpa cylindracea*
122 were analyzed. In addition, 18 samples (one of the samples was sequenced two times) originating
123 from picoplankton archaeal and bacterial communities in the surrounding seawater were also

124 processed. The number of reads per sample ranged between 8,407 and 77,465 sequences
125 (Table S1). Even when the highest sequencing effort was applied the rarefaction curves did
126 not level off that is a common observation in high-throughput 16S rRNA amplicon sequencing
127 approaches (Figure S1). Following quality curation and exclusion of sequences mentioned before
128 reads were clustered into 28,726 different OTUs at a similarity level of 97 %. Reads numbers
129 were normalized to the minimum number of sequences, 8,407 (Table S1), through rarefaction
130 resulting in 17,020 different OTUs that ranged from 346 to 2,010 OTUs per sample (Figure S2).

131 To determine seasonal changes of richness and diversity the Observed Number of OTUs, Chao1,
132 ACE, Exponential Shannon (Jost, 2006) and Inverse Simpson were calculated after normalization
133 through rarefaction. Generally, richness estimators and diversity indices showed similar trends. On
134 average, higher values were found for *Caulerpa cylindracea* (invaded [Number of OTUs, 1,693.5
135 \pm 122.3 OTUs] and noninvaded [Number of OTUs, 1,745.5 \pm 150.9 OTUs]), middle values for
136 *Cymodocea nodosa* (Number of OTUs, 1,056.7 \pm 212.5 OTUs) and lower values for picoplankton
137 communities in the surrounding seawater (Number of OTUs, 531.7 \pm 142.7 OTUs) (Figure S2).
138 Seasonal changes did not show such large dissimilarities. Seawater communities richness was
139 stable during the studied period with the exception of one sampling point in December 2017
140 when larger values were observed. *Cymodocea nodosa* communities showed a slow increase
141 towards the end of the study, while *Caulerpa cylindracea* (invaded and noninvaded) communities
142 were characterized by slightly larger values in Spring and Summer in comparison to Autumn and
143 Winter (Figure S2).

144 To determine the proportion of shared archaeal and bacterial OTUs and communities sampled
145 in different environments the Jaccard's Similarity Coefficient on presence-absence data and
146 Bray-Curtis Similarity Coefficient were, respectively, calculated. Coefficients were determined
147 after normalization through rarefaction and binning of samples from a particular environment. The
148 highest proportion of shared OTUs and community was found between invaded and noninvaded
149 *Caulerpa cylindracea* (Jaccard, 0.36; Bray-Curtis, 0.77), while lower shared values were
150 calculated between seawater and epiphytic communities (Figure 1). Shared proportion between

151 *Cymodocea nodosa* and *Caulerpa cylindracea* were approximately in the middle between these
152 two extremes. To assess seasonal changes in the proportion of shared OTUs and communities the
153 Jaccard's and Bray-Curtis Similarity Coefficients were calculated between consecutive sampling
154 points (Figure 2). Both coefficients showed similar trends. Temporal proportional changes were
155 more pronounced for seawater in comparison to *Cymodocea nodosa* and especially *Caulerpa*
156 *cylindracea* associated communities (Figure 2). To further disentangle the environmental and
157 seasonal community dissimilarity a Principal Coordinates Analysis (PCoA) based on Bray-Curtis
158 distances and OTU abundances was applied. It showed a clear separation between planktonic
159 and surface associated communities (Figure 3). In addition, a separation of epiphytic bacterial
160 and archaeal communities based on host species was determined. This separation was further
161 supported by ANOSIM ($R = 0.96, p < 0.001$). Seasonal changes of seawater communities
162 indicated a separation between Spring, Summer and Autumn/Winter samples (ANOSIM, $R =$
163 $0.63, p < 0.001$). Epiphytic microbial communities associated with *Cymodocea nodosa* showed a
164 similar pattern (ANOSIM, $R = 0.54, p < 0.001$), while communities from the surfaces of *Caulerpa*
165 *cylindracea* indicated a non so strongly supported, as in previous cases, separation between
166 Summer and Autumn/Winter/Spring samples (ANOSIM, $R = 0.31, p < 0.05$) (Figure 3).

167 The taxonomic composition of both, macrophyte associated and seawater communities,
168 was dominated by *Bacteria* ($99.1 \pm 2.1 \%$) over *Archaea* ($0.9 \pm 2.1 \%$) (Figure 4). Higher
169 relative abundances of chloroplast related sequences were only observed in surface associated
170 communities, with higher values in Autumn/Winter ($37.2 \pm 11.2 \%$) in comparison to
171 Spring/Summer ($20.9 \pm 9.7 \%$) (Figure S3). Generally, at higher taxonomic ranks (phylum-class)
172 epiphytic and seawater microbial communities were composed of similar bacterial taxa.
173 Seawater communities were mainly comprised of *Actinobacteriota*, *Bacteroidota*, *Cyanobacteria*,
174 *Alphaproteobacteria*, *Gammaproteobacteria* and *Verrucomicrobiota*. Communities associated
175 with *Cymodocea nodosa* were consisted of same groups with the addition of *Planctomycetota*
176 whose contribution was higher in summer 2018. In addition, communities from invaded and
177 noninvaded *Caulerpa cylindracea* were similar and characterized by same groups as seawater

178 and *Cymodocea nodosa* communities with the addition of *Desulfobacterota* (Figure 4). Larger
179 differences between environments and host species could be observed at lower taxonomic ranks
180 (Figure 5 – 9).

181 *Cyanobacteria* related sequences were comprising, on average, 5.5 ± 4.4 % of total sequences
182 (Figure 5). Higher proportions were found for *Cymodocea nodosa* (16.4 ± 5.3 %) and *Caulerpa*
183 *cylindracea* (invaded [7.7 ± 3.9 %]) and noninvaded [$(7.8 \pm 2.4$ %)]) associated communities
184 in autumn and for seawater communities in winter (8.8 ± 7.4 %). Large taxonomic differences
185 between surface associated and seawater cyanobacterial communities were observed. Seawater
186 communities were mainly comprised of *Cyanobium* and *Synechococcus*, while surface associated
187 communities were consisted of *Pleurocapsa* and sequences without known relatives within
188 *Cyanobacteriia* (Figure 5). In addition, seasonal changes in surface associated communities
189 were observed with *Pleurocapsa* and no relative *Cyanobacteriia* comprising larger proportions in
190 autumn and winter and *Acrophormium*, *Phormidesmis* and no relative *Nodosilineaceae* in spring
191 and summer (Figure 5).

192 Sequences classified as *Bacteroidota* were comprising, on average, 19.2 ± 5.5 % of all
193 sequences (Figure 6). Similarly to *Cyanobacteria*, large differences in the taxonomic composition
194 between seawater and surface associated communities were found (Figure 6). The seawater
195 community was characterized by the NS4 and NS5 marine groups, uncultured *Cryomorphaceae*,
196 uncultured *Flavobacteriaceae*, NS11-12 marine group, *Balneola*, uncultured *Balneolaceae* and
197 *Formosa*. In contrast, in surface associated communities *Lewinella*, *Portibacter*, *Rubidimonas*, no
198 relative *Saprospiraceae*, uncultured *Saprospiraceae*, no relative *Flavobacteriaceae* and uncultured
199 *Rhodothermaceae* were found. Some groups showed slight seasonal changes such as no relative
200 *Flavobacteriaceae* that were more pronounced from November 2017 until June 2018. In contrast,
201 uncultured *Rhodothermaceae* showed higher proportions from June 2018 until the end of the study
202 period. Surface associated *Bacteroidota* communities were very diverse as could be observed in
203 the the high proportion of taxa that grouped as other *Bacteroidota* (Figure 6).

204 On average, *Alphaproteobacteria* were in comparison to other high rank taxa the largest
205 taxonomic group, comprising 29.2 ± 12.0 % of all sequences (Figure 7). In accordance to previous
206 taxa, high differences between seawater and surface associated communities were observed.
207 Picoplankton communities were composed mainly of the SAR11 clade, AEGEAN-169 marine
208 group, SAR116 clade, no relative *Rhodobacteraceae*, HIMB11 and OCS116 clade, while surface
209 associated communities were composed in high proportion of no relative *Rhodobacteraceae* and to
210 a lesser degree of *Pseudoahrensia*, no relative *Alphaproteobacteria*, no relative *Hyphomonadaceae*
211 and *Amylibacter*. Representatives of no relative *Rhodobacteraceae* were comprising on average
212 40.6 ± 23.2 % of all alphaproteobacterial sequences from the epiphytic community (Figure 7).
213 In addition, *Amylibacter* was detected mainly in *Cymodocea nodosa* from November 2017 until
214 March 2018.

215 Sequences related to *Gammaproteobacteria* were comprising, on average, 18.7 ± 3.9 % of all
216 sequences (Figure 8). Similarly to previous taxa, large taxonomic differences between seawater
217 and surface associated communities were found. Seawater communities were mainly comprised
218 of the OM60 (NOR5) clade, *Litoricola*, *Acinetobacter* and the SAR86 clade, while epiphytic
219 communities were mainly composed of no relative *Gammaproteobacteria* and *Granulosicoccus*.
220 Beside these two groups specific to all three epiphytic communities, *Cymodocea nodosa* was
221 characterized by *Arenicella*, no relative *Burkholderiales* and *Methylotenera*, while *Thioploca*,
222 no relative *Cellvibrionaceae* and *Reinekea* were more specific to both invaded and noninvaded
223 *Caulerpa cylindracea*. In addition, *Arenicella* was more pronounced in November and December
224 2017, while no relative *Burkholderiales* and *Methylotenera* were more characteristic for the
225 period form March until May 2018. For the *Caulerpa cylindracea* specific taxa no relative
226 *Cellvibrionaceae* and *Reinekea* showed some seasonality and were characterisitic for samples
227 originating from June to October 2018. In addition, similarly to *Bacteroidota*, a large proportion
228 of the surface associated community was grouped as other *Gammaproteobacteria* indicating high
229 diversity within this group (Figure 8).

230 In contrast to previously described high rank taxa, *Desulfobacterota* were specific to
231 *Caulerpa cylindracea*. On average they were comprising 11.2 ± 13.3 % of all sequences. While
232 seawater and *Cymodocea nodosa* communities were consisted of only 0.1 ± 0.08 % and 1.0
233 ± 0.7 % *Desulfobacterota* sequences, respectively, in the invaded and noninvaded *Caulerpa*
234 *cylindracea* communities their proportion was 25.7 ± 11.3 % and 24.0 ± 4.3 %, respectively
235 (Figure 9). In addition, *Caulerpa cylindracea* associated communities were characterized by
236 higer proportions in Winter and Summer (invaded, 30.9 ± 12.4 %; noninvaded, 26.9 ± 3.4 %)
237 in comparison to Autumn and Spring (invaded, 22.8 ± 10.3 %; noninvaded, 21.9 ± 3.8 %). The
238 community was mainly consisted of no relative *Desulfobacteraceae*, *Desulfatitalea*, no relative
239 *Desulfobulbaceae*, *Desulfobulbus*, no relative *Desulfocapsaceae*, *Desulfopila*, *Desulforhopalus*,
240 *Desulfotalea*, SEEP-SRB4 and uncultured *Desulfocapsaceae* (Figure 9).

241 Discussion

242 Surfaces of marine macrophytes are harboring biofilms consisted of diverse microbial taxa
243 (Egan *et al.*, 2013; Tarquinio *et al.*, 2019). No standard protocol has been developed to study
244 these macophyte associated microbes (Ugarelli *et al.*, 2019). Different procedures of microbial
245 cells removal from host surfaces were described, such as host tissue shaking (Nõges *et al.*, 2010),
246 scraping (Uku *et al.*, 2007) and ultrasonication (Cai *et al.*, 2014). All these methods showed
247 different removal efficiencies and none was enabling a complete removal of attached microbial
248 cells. In the present study, we applied an earlier developed removal protocol (Korlević *et al.*,
249 submitted), based on a previous idea of direct cellular lysis (Burke *et al.*, 2009), to ensure an
250 almost complete cell detachment. The application of a direct lysis procedure coupled with a high
251 frequency sampling protocol and Illumina high resolution amplicon sequencing has enabled us to
252 make a detailed description of bacterial and archaeal communities associated with the surfaces of
253 two marine macrophytes, *Cymodocea nodosa* and *Caulerpa cylindracea*.

254 Observed highest richness values for *Caulerpa cylindracea* (invaded and noninvaded),
255 middle for *Cymodocea nodosa* and lowest for seawater derived communities. Higher values for
256 surface associated communities in comparison to seawater were described earlier for seagrasses
257 (Ugarelli *et al.*, 2019) and could be attributed to a larger set of inhabitable microniches existing
258 on macrophyte surfaces. In addition, highest values observed for *Caulerpa cylindracea* are
259 probably a consequence of sediment derived OTUs that were present only in *Caulerpa cylindracea*
260 communities. *Caulerpa cylindracea* stolon is attached to surface sediment with rhizoids, so the
261 stolon and rhizoids are in a direct contact with the sediment surface. Part of the surface attached
262 *Caulerpa cylindracea* community is therefore comprised of sediment derived cells that could
263 cause the observed increase in richness. In addition, seasonal richness differences observed for
264 surface attached communities showed slightly higher values in spring and summer could be
265 explained by a higher macrophyte growth in these seasons (M. Najdek, personal communication;
266 Zavodnik *et al.*, 1998; Ruitton *et al.*, 2005). During active periods macrophytes exhibit a more
267 dynamic chemical interaction with the surface community causing an opening of a larger set of
268 microniches.

269 **Acknowledgments**

270 **References**

- 271 Allaire, J.J., Xie, Y., McPherson, J., Luraschi, J., Ushey, K., Atkins, A., et al. (2019)
- 272 rmarkdown: Dynamic Documents for R.
- 273 Apprill, A., McNally, S., Parsons, R., and Weber, L. (2015) Minor revision to V4 region
- 274 SSU rRNA 806R gene primer greatly increases detection of SAR11 bacterioplankton. *Aquatic*
- 275 *Microbial Ecology* **75**: 129–137.
- 276 Armstrong, E., Rogerson, A., and Leftley, J. (2000) The Abundance of Heterotrophic Protists
- 277 Associated with Intertidal Seaweeds. *Estuarine, Coastal and Shelf Science* **50**: 415–424.
- 278 Bengtsson, M., Sjøtun, K., and Øvreås, L. (2010) Seasonal dynamics of bacterial biofilms on
- 279 the kelp *Laminaria hyperborea*. *Aquatic Microbial Ecology* **60**: 71–83.
- 280 Burke, C., Kjelleberg, S., and Thomas, T. (2009) Selective extraction of bacterial DNA from
- 281 the surfaces of macroalgae. *Applied and environmental microbiology* **75**: 252–256.
- 282 Burke, C., Steinberg, P., Rusch, D., Kjelleberg, S., and Thomas, T. (2011a) Bacterial
- 283 community assembly based on functional genes rather than species. *Proceedings of the National*
- 284 *Academy of Sciences of the United States of America* **108**: 14288–14293.
- 285 Burke, C., Thomas, T., Lewis, M., Steinberg, P., and Kjelleberg, S. (2011b) Composition,
- 286 uniqueness and variability of the epiphytic bacterial community of the green alga *Ulva australis*.
- 287 *The ISME journal* **5**: 590–600.
- 288 Cai, X., Gao, G., Yang, J., Tang, X., Dai, J., Chen, D., and Song, Y. (2014) An ultrasonic
- 289 method for separation of epiphytic microbes from freshwater submerged macrophytes. *Journal of*
- 290 *basic microbiology* **54**: 758–761.
- 291 Caporaso, J.G., Lauber, C.L., Walters, W.A., Berg-Lyons, D., Huntley, J., Fierer, N., et al.

292 (2012) Ultra-high-throughput microbial community analysis on the Illumina HiSeq and MiSeq
293 platforms. *The ISME Journal* **6**: 1621–1624.

294 Crump, B.C. and Koch, E.W. (2008) Attached bacterial populations shared by four species of
295 aquatic angiosperms. *Applied and environmental microbiology* **74**: 5948–5957.

296 Egan, S., Harder, T., Burke, C., Steinberg, P., Kjelleberg, S., and Thomas, T. (2013) The
297 seaweed holobiont: understanding seaweed-bacteria interactions. *FEMS microbiology reviews* **37**:
298 462–476.

299 Hollants, J., Leliaert, F., De Clerck, O., and Willems, A. (2013) What we can learn from
300 sushi: A review on seaweed-bacterial associations. *83*: 1–16.

301 Jost, L. (2006) Entropy and diversity. *113*: 363–375.

302 Korlević, M., Markovski, M., Zhao, Z., Herndl, G.J., and Najdek, M. Selective DNA and
303 Protein Isolation from Marine Macrophyte Surfaces.

304 Kozich, J.J., Westcott, S.L., Baxter, N.T., Highlander, S.K., and Schloss, P.D. (2013)
305 Development of a dual-index sequencing strategy and curation pipeline for analyzing amplicon
306 sequence data on the MiSeq Illumina sequencing platform. *Applied and environmental*
307 *microbiology* **79**: 5112–5120.

308 Lachnit, T., Blümel, M., Imhoff, J.F., and Wahl, M. (2009) Specific epibacterial communities
309 on macroalgae: Phylogeny matters more than habitat. *Aquatic Biology* **5**: 181–186.

310 Lachnit, T., Meske, D., Wahl, M., Harder, T., and Schmitz, R. (2011) Epibacterial community
311 patterns on marine macroalgae are host-specific but temporally variable. *Environmental*
312 *Microbiology* **13**: 655–665.

313 Margulis, L. (1991) Symbiogenesis and symbiontism. In, Margulis,L. and Fester,R. (eds),
314 *Symbiosis as a source of evolutionary innovation*. Cambridge, Massachusetts: The MIT Press, pp.

315 1–14.

316 Massana, R., Murray, A.E., Preston, C.M., and DeLong, E.F. (1997) Vertical distribution and
317 phylogenetic characterization of marine planktonic Archaea in the Santa Barbara Channel. *Applied*
318 *and environmental microbiology* **63**: 50–56.

319 Miranda, L.N., Hutchison, K., Grossman, A.R., and Brawley, S.H. (2013) Diversity and
320 Abundance of the Bacterial Community of the Red Macroalga *Porphyra umbilicalis*: Did Bacterial
321 Farmers Produce Macroalgae? *PLoS ONE* **8**: e58269.

322 Morrissey, K.L., Çavas, L., Willems, A., and De Clerck, O. (2019) Disentangling the influence
323 of environment, host specificity and thallus differentiation on bacterial communities in siphonous
324 green seaweeds. *Frontiers in Microbiology* **10**:

325 Neuwirth, E. (2014) RColorBrewer: ColorBrewer Palettes.

326 Nõges, T., Luup, H., and Feldmann, T. (2010) Primary production of aquatic macrophytes
327 and their epiphytes in two shallow lakes (Peipsi and Võrtsjärv) in Estonia. *Aquatic Ecology* **44**:
328 83–92.

329 Oksanen, J., Blanchet, F.G., Friendly, M., Kindt, R., Legendre, P., McGlinn, D., et al. (2019)
330 vegan: Community Ecology Package.

331 Parada, A.E., Needham, D.M., and Fuhrman, J.A. (2016) Every base matters: assessing small
332 subunit rRNA primers for marine microbiomes with mock communities, time series and global
333 field samples. *Environmental Microbiology* **18**: 1403–1414.

334 Quast, C., Pruesse, E., Yilmaz, P., Gerken, J., Schweer, T., Yarza, P., et al. (2013) The SILVA
335 ribosomal RNA gene database project: improved data processing and web-based tools. *Nucleic*
336 *acids research* **41**: D590–6.

337 R Core Team (2019) R: A Language and Environment for Statistical Computing, Vienna,

- 338 Austria: R Foundation for Statistical Computing.
- 339 Roth-Schulze, A.J., Zozaya-Valdés, E., Steinberg, P.D., and Thomas, T. (2016) Partitioning of
340 functional and taxonomic diversity in surface-associated microbial communities. *Environmental*
341 *microbiology* **18**: 4391–4402.
- 342 Ruitton, S., Verlaque, M., and Boudouresque, C.F. (2005) Seasonal changes of the introduced
343 *Caulerpa racemosa* var. *cylindracea* (Caulerpales, Chlorophyta) at the northwest limit of its
344 Mediterranean range. *Aquatic Botany* **82**: 55–70.
- 345 Schloss, P.D., Girard, R.A., Martin, T., Edwards, J., and Thrash, J.C. (2016) Status of the
346 Archaeal and Bacterial Census: an Update. *mBio* **7**: e00201–16.
- 347 Schloss, P.D., Westcott, S.L., Ryabin, T., Hall, J.R., Hartmann, M., Hollister, E.B., et al.
348 (2009) Introducing mothur: open-source, platform-independent, community-supported software
349 for describing and comparing microbial communities. *Applied and environmental microbiology*
350 **75**: 7537–7541.
- 351 Tarquinio, F., Hyndes, G.A., Laverock, B., Koenders, A., and Säwström, C. (2019) The
352 seagrass holobiont: Understanding seagrass-bacteria interactions and their role in seagrass
353 ecosystem functioning. *FEMS Microbiology Letters* **366**:
- 354 Tujula, N.A., Crocetti, G.R., Burke, C., Thomas, T., Holmström, C., and Kjelleberg, S. (2010)
355 Variability and abundance of the epiphytic bacterial community associated with a green marine
356 Ulvacean alga. *The ISME Journal* **4**: 301–311.
- 357 Ugarelli, K., Laas, P., and Stingl, U. (2019) The microbial communities of leaves and roots
358 associated with turtle grass (*Thalassia testudinum*) and manatee grass (*syringodium filiforme*) are
359 distinct from seawater and sediment communities, but are similar between species and sampling
360 sites. *Microorganisms* **7**:

361 Uku, J., Björk, M., Bergman, B., and Díez, B. (2007) Characterization and comparison of
362 prokaryotic epiphytes associated with three East African seagrasses. *Journal of Phycology* **43**:
363 768–779.

364 Wickham, H., Averick, M., Bryan, J., Chang, W., McGowan, L.D., François, R., et al. (2019)
365 Welcome to the tidyverse. *Journal of Open Source Software* **4**: 1686.

366 Xie, Y. (2015) Dynamic Documents with {R} and knitr, 2nd ed. Boca Raton, Florida:
367 Chapman; Hall/CRC.

368 Xie, Y. (2014) knitr: A Comprehensive Tool for Reproducible Research in {R}. In,
369 Stodden, V., Leisch, F., and Peng, R.D. (eds), *Implementing reproducible computational research*.
370 Chapman; Hall/CRC.

371 Xie, Y. (2019a) knitr: A General-Purpose Package for Dynamic Report Generation in R.

372 Xie, Y. (2019b) TinyTeX: A lightweight, cross-platform, and easy-to-maintain LaTeX
373 distribution based on TeX Live. *TUGboat* 30–32.

374 Xie, Y. (2020) tinytex: Helper Functions to Install and Maintain 'TeX Live', and Compile
375 'LaTeX' Documents.

376 Xie, Y., Allaire, J.J., and Grolemund, G. (2018) R Markdown: The Definitive Guide, Boca
377 Raton, Florida: Chapman; Hall/CRC.

378 Yilmaz, P., Parfrey, L.W., Yarza, P., Gerken, J., Pruesse, E., Quast, C., et al. (2014) The SILVA
379 and "All-species Living Tree Project (LTP)" taxonomic frameworks. *Nucleic acids research* **42**:
380 D643–8.

381 Zavodnik, N., Travizi, A., and De Rosa, S. (1998) Seasonal variations in the rate of
382 pliotosynthetic activity and chemical composition of the seagrass *Cymodocea nodosa* (Ucr.) Asch.
383 *Scientia Marina* **62**: 301–309.

Zhu, H. (2019) *kableExtra: Construct Complex Table with 'kable' and Pipe Syntax*.

385 **Figure Captions**

386 **Figure 1.** Proportion of shared bacterial and archaeal OTUs (Jaccard's Similarity Coefficient)
387 and shared bacterial and archaeal communities (Bray-Curtis Similarity Coefficient) between
388 communities associated with the surfaces of macrophytes (*Cymodocea nodosa* [Invaded] and
389 *Caulerpa cylindracea* [Invaded and Noninvaded]) and coomunities in the surrounding seawater.

390 **Figure 2.** Proportion of shared bacterial and archaeal communities (Bray-Curtis Similarity
391 Coefficient) and shared bacterial and archaeal OTUs (Jaccard's Similarity Coefficient) between
392 consecutive sampling points and from the surfaces of macrophytes (*Cymodocea nodosa* [Invaded]
393 and *Caulerpa cylindracea* [Invaded and Noninvaded]) and in the surrounding seawater.

394 **Figure 3.** Principal Coordinates Analysis (PCoA) of Bray-Curtis distances based on OTU
395 abundances of bacterial and archaeal communities from the surfaces of macrophytes (*Cymodocea*
396 *nodosa* [Invaded] and *Caulerpa cylindracea* [Invaded and Noninvaded]) and in the surrounding
397 seawater. Samples from the same environment or same season are labeld in different colors. The
398 proportion of explained variation by each axis is shown on the corresponding axis in parentheses.

399 **Figure 4.** Taxonomic classification and relative contribution of the most abundant bacterial and
400 archaeal sequences on the surfaces of macrophytes (*Cymodocea nodosa* [Invaded] and *Caulerpa*
401 *cylindracea* [Invaded and Noninvaded]) and in the surrounding seawater.

402 **Figure 5.** Taxonomic classification and relative contribution of the most abundant cyanobacterial
403 sequences on the surfaces of macrophytes (*Cymodocea nodosa* [Invaded] and *Caulerpa*
404 *cylindracea* [Invaded and Noninvaded]) and in the surrounding seawater. The proportion of
405 cyanobacterial sequences in the total bacterial and archaeal community is given above the
406 corresponding bar. NR – No Relative

407 **Figure 6.** Taxonomic classification and relative contribution of the most abundant sequences
408 within the *Bacteroidota* on the surfaces of macrophytes (*Cymodocea nodosa* [Invaded] and

409 *Caulerpa cylindracea* [Invaded and Noninvaded]) and in the surrounding seawater. The proportion
410 of sequences classified as *Bacteroidota* in the total bacterial and archaeal community is given
411 above the corresponding bar. NR – No Relative

412 **Figure 7.** Taxonomic classification and relative contribution of the most abundant alphaproteobacterial
413 sequences on the surfaces of macrophytes (*Cymodocea nodosa* [Invaded] and *Caulerpa*
414 *cylindracea* [Invaded and Noninvaded]) and in the surrounding seawater. The proportion of
415 alphaproteobacterial sequences in the total bacterial and archaeal community is given above the
416 corresponding bar. NR – No Relative

417 **Figure 8.** Taxonomic classification and relative contribution of the most abundant gammaproteobacterial
418 sequences on the surfaces of macrophytes (*Cymodocea nodosa* [Invaded] and *Caulerpa*
419 *cylindracea* [Invaded and Noninvaded]) and in the surrounding seawater. The proportion of
420 gammaproteobacterial sequences in the total bacterial and archaeal community is given above the
421 corresponding bar. NR – No Relative

422 **Figure 9.** Taxonomic classification and relative contribution of the most abundant sequences
423 within the *Desulfobacterota* on the surfaces of macrophytes (*Cymodocea nodosa* [Invaded] and
424 *Caulerpa cylindracea* [Invaded and Noninvaded]) and in the surrounding seawater. The proportion
425 of sequences classified as *Desulfobacterota* in the total bacterial and archaeal community is given
426 above the corresponding bar. NR – No Relative

427 **Figures**

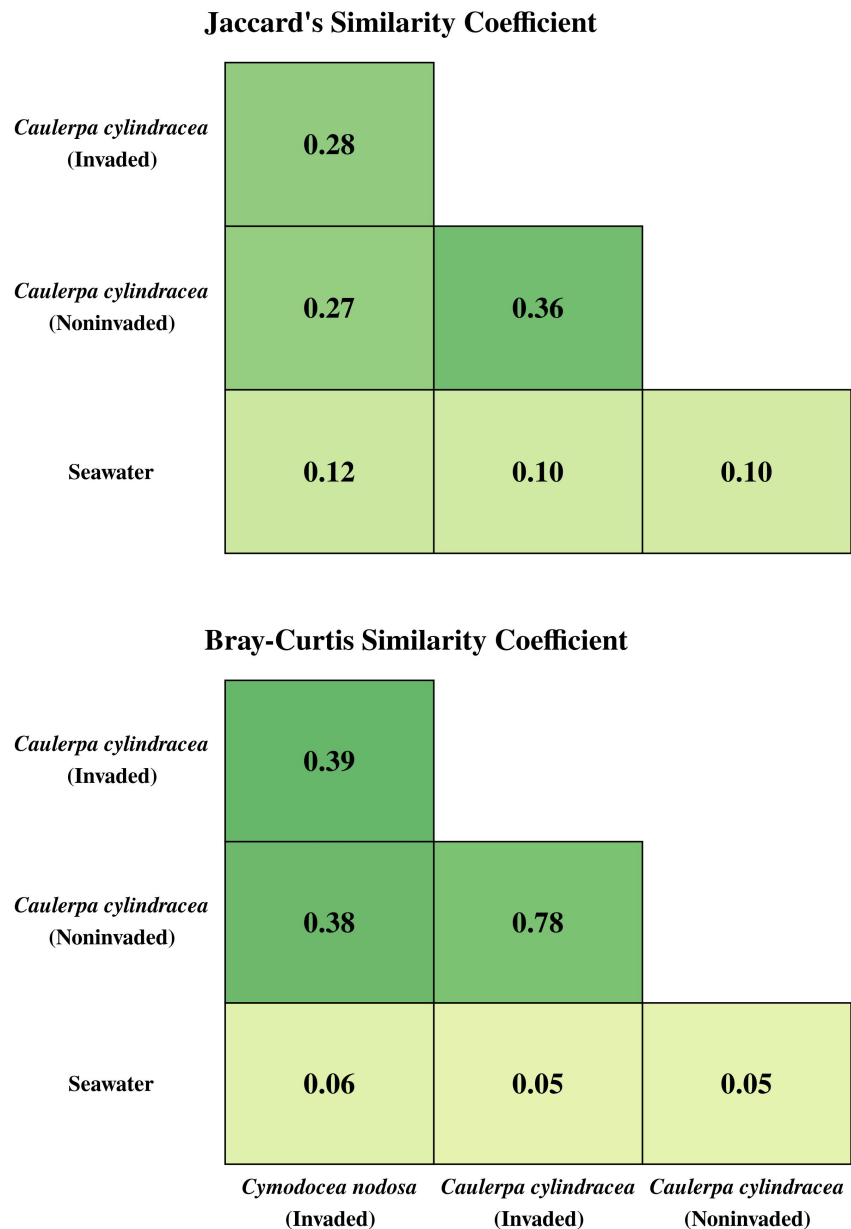


Figure 1. Proportion of shared bacterial and archaeal OTUs (Jaccard's Similarity Coefficient) and shared bacterial and archaeal communities (Bray-Curtis Similarity Coefficient) between communities associated with the surfaces of macrophytes (*Cymodocea nodosa* [Invaded] and *Caulerpa cylindracea* [Invaded and Noninvaded]) and coomunities in the surrounding seawater.

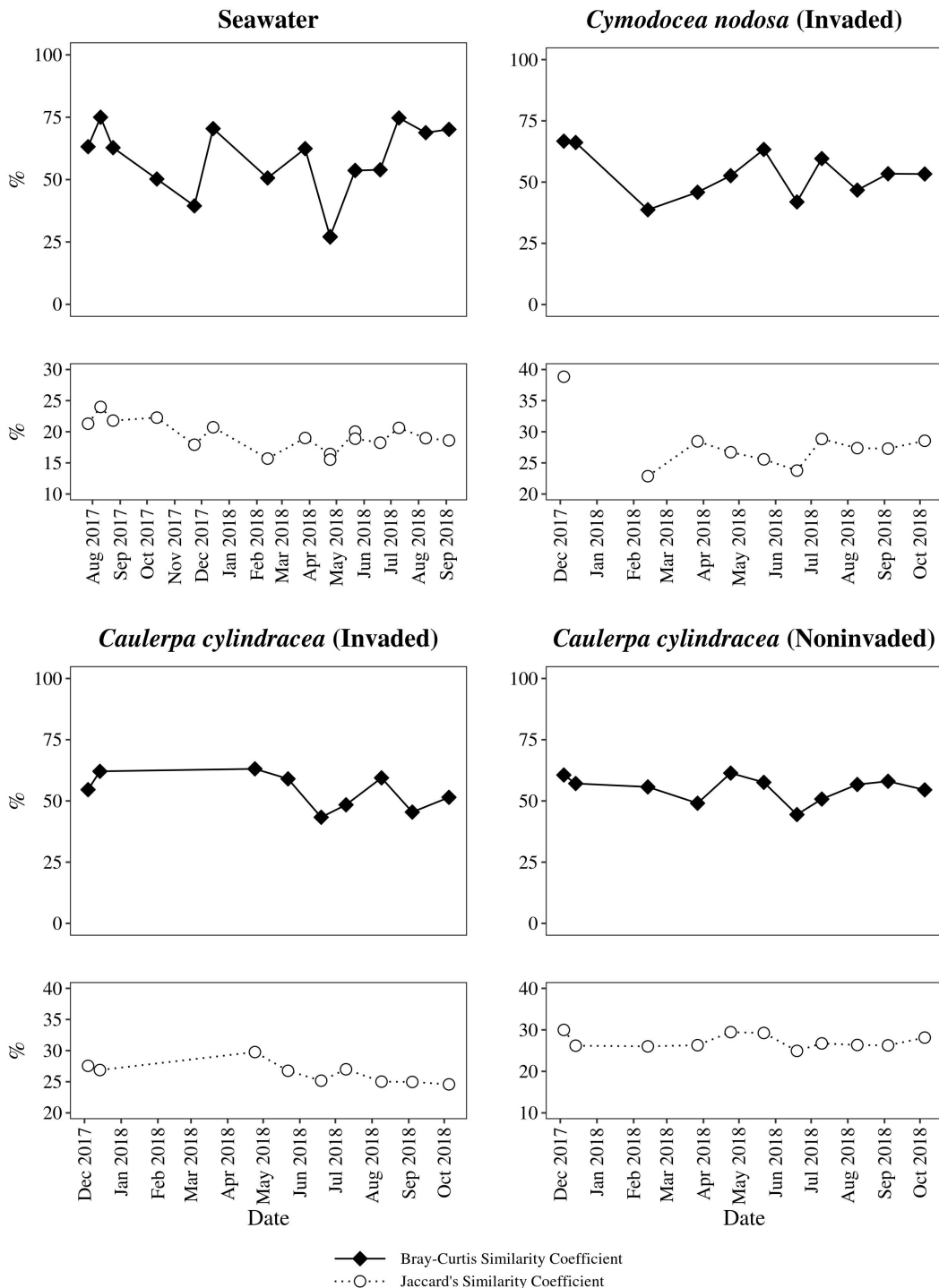


Figure 2. Proportion of shared bacterial and archaeal communities (Bray-Curtis Similarity Coefficient) and shared bacterial and archaeal OTUs (Jaccard's Similarity Coefficient) between consecutive sampling points and from the surfaces of macrophytes (*Cymodocea nodosa* [Invaded] and *Caulerpa cylindracea* [Invaded and Noninvaded]) and in the surrounding seawater.

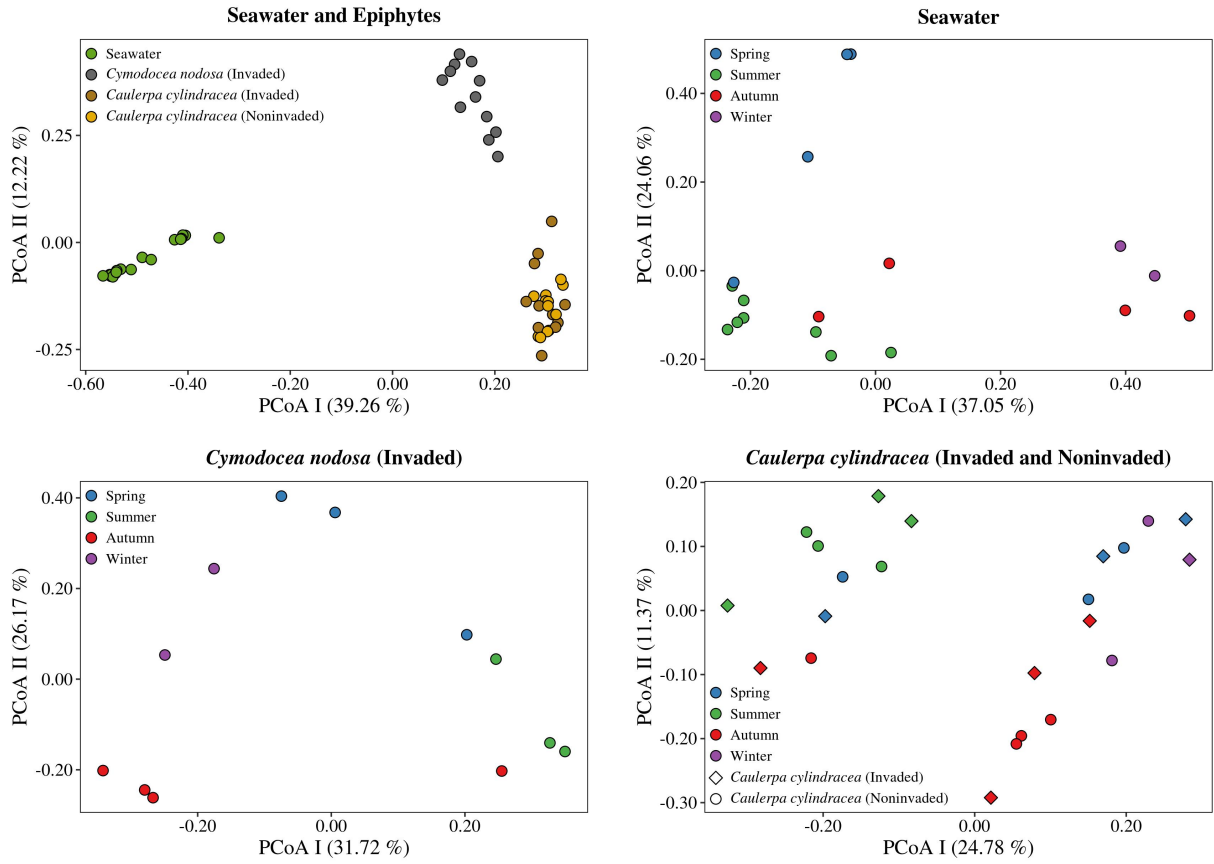


Figure 3. Principal Coordinates Analysis (PCoA) of Bray-Curtis distances based on OTU abundances of bacterial and archaeal communities from the surfaces of macrophytes (*Cymodocea nodosa* [Invaded] and *Caulerpa cylindracea* [Invaded and Noninvaded]) and in the surrounding seawater. Samples from the same environment or same season are labeled in different colors. The proportion of explained variation by each axis is shown on the corresponding axis in parentheses.

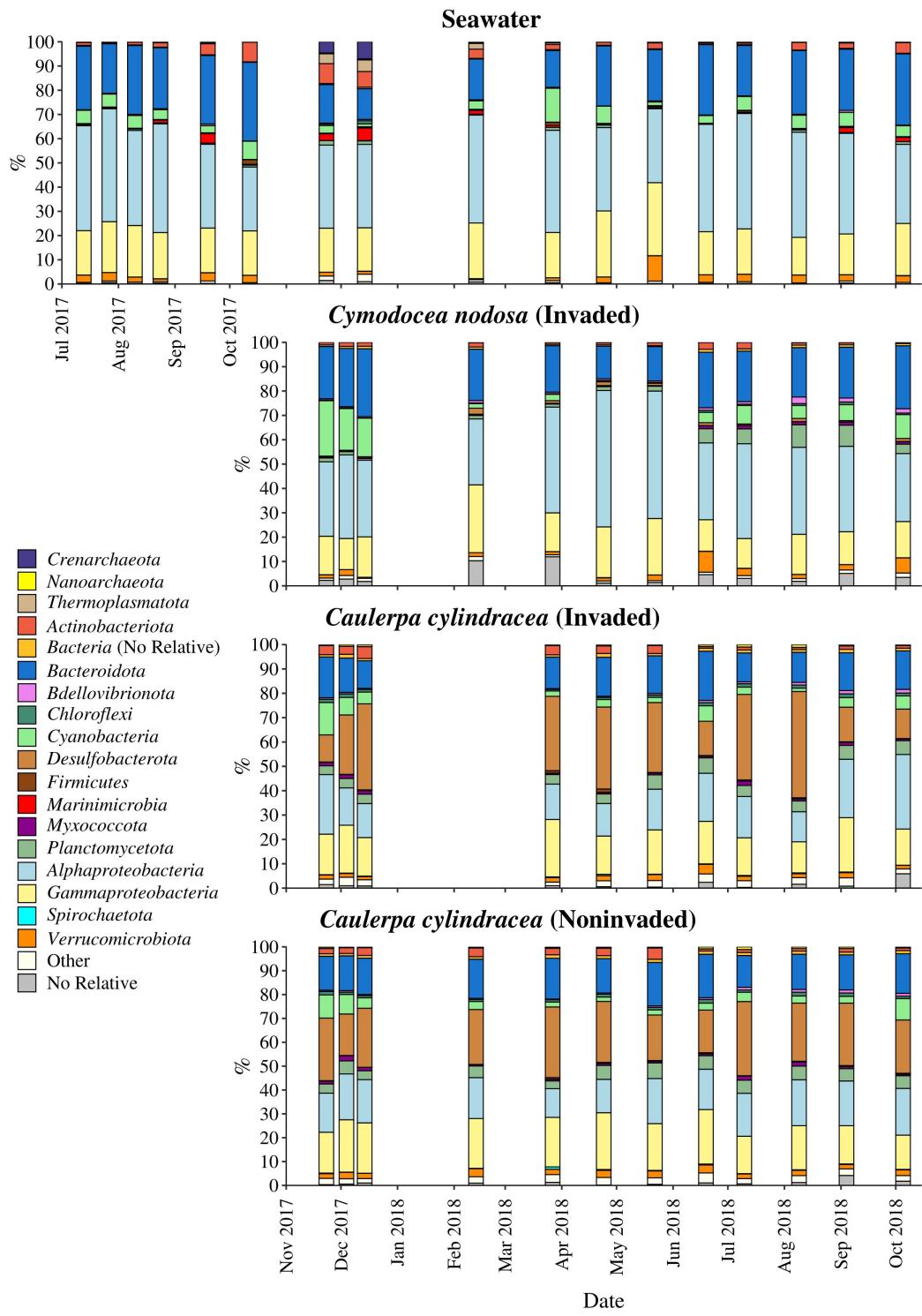


Figure 4. Taxonomic classification and relative contribution of the most abundant bacterial and archaeal sequences on the surfaces of macrophytes (*Cymodocea nodosa* [Invaded] and *Caulerpa cylindracea* [Invaded and Noninvaded]) and in the surrounding seawater.

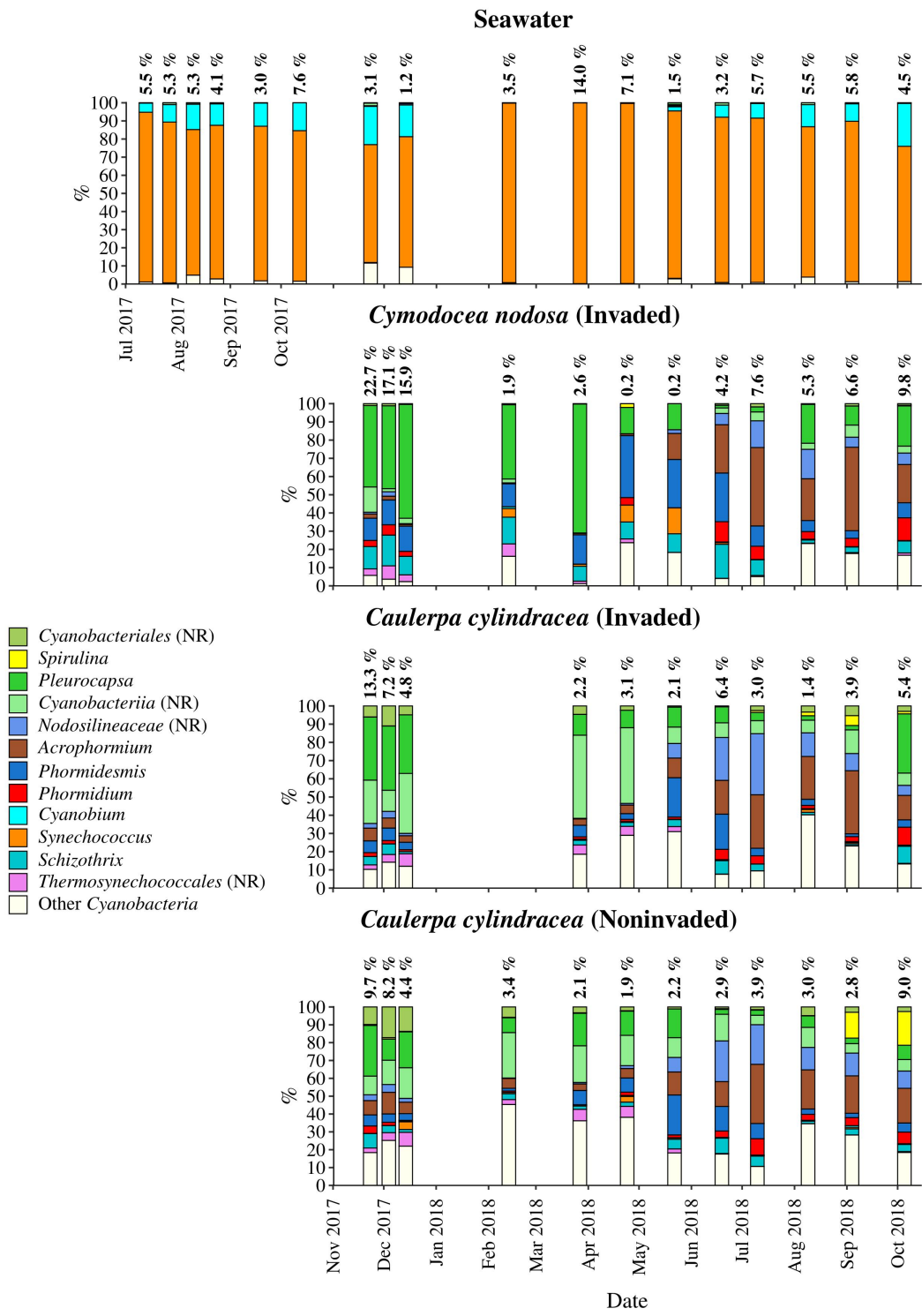


Figure 5. Taxonomic classification and relative contribution of the most abundant cyanobacterial sequences on the surfaces of macrophytes (*Cymodocea nodosa* [Invaded] and *Caulerpa cylindracea* [Invaded and Noninvaded]) and in the surrounding seawater. The proportion of cyanobacterial sequences in the total bacterial and archaeal community is given above the corresponding bar. NR – No Relative

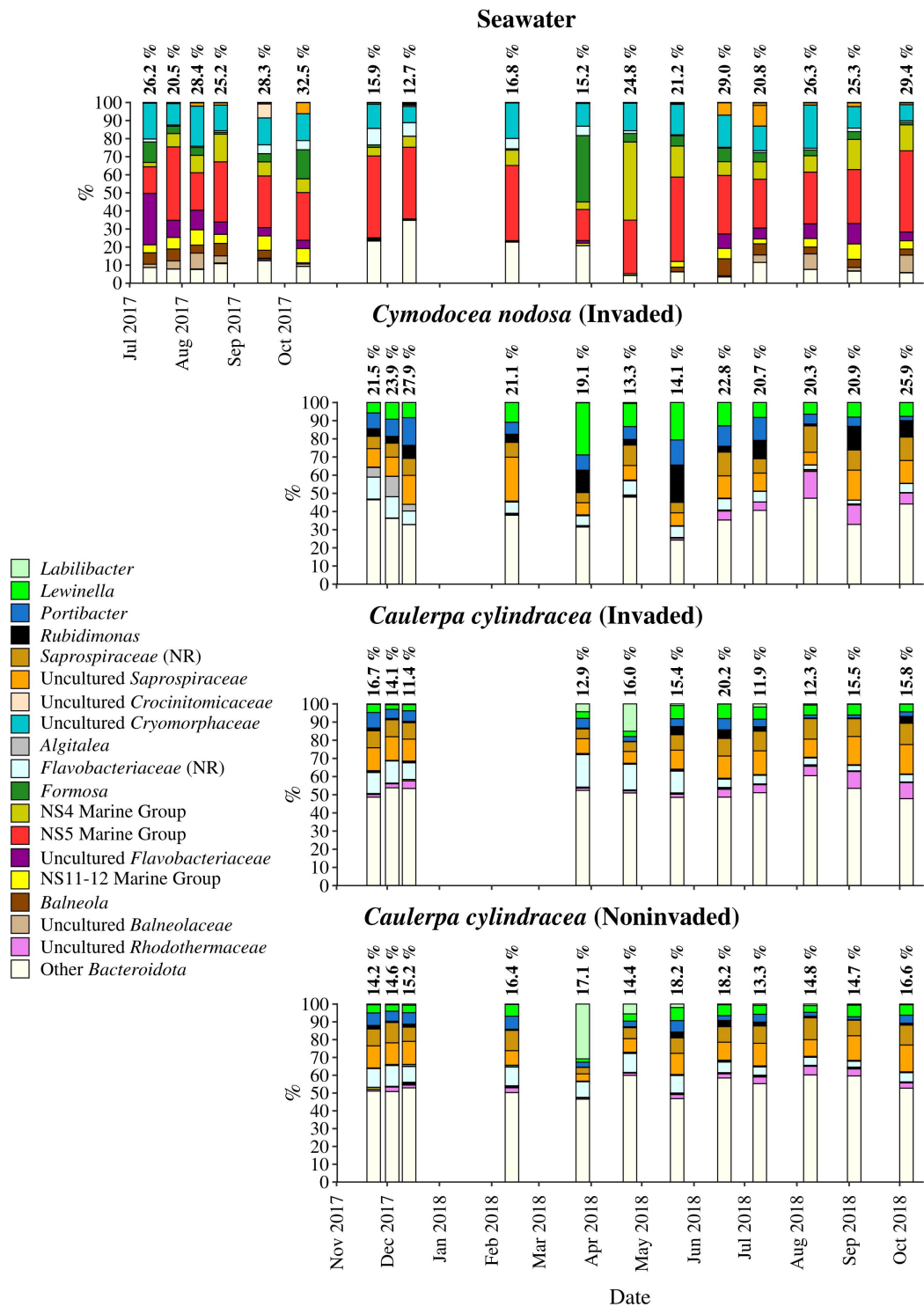


Figure 6. Taxonomic classification and relative contribution of the most abundant sequences within the *Bacteroidota* on the surfaces of macrophytes (*Cymodocea nodosa* [Invaded] and *Caulerpa cylindracea* [Invaded and Noninvaded]) and in the surrounding seawater. The proportion of sequences classified as *Bacteroidota* in the total bacterial and archaeal community is given above the corresponding bar. NR – No Relative

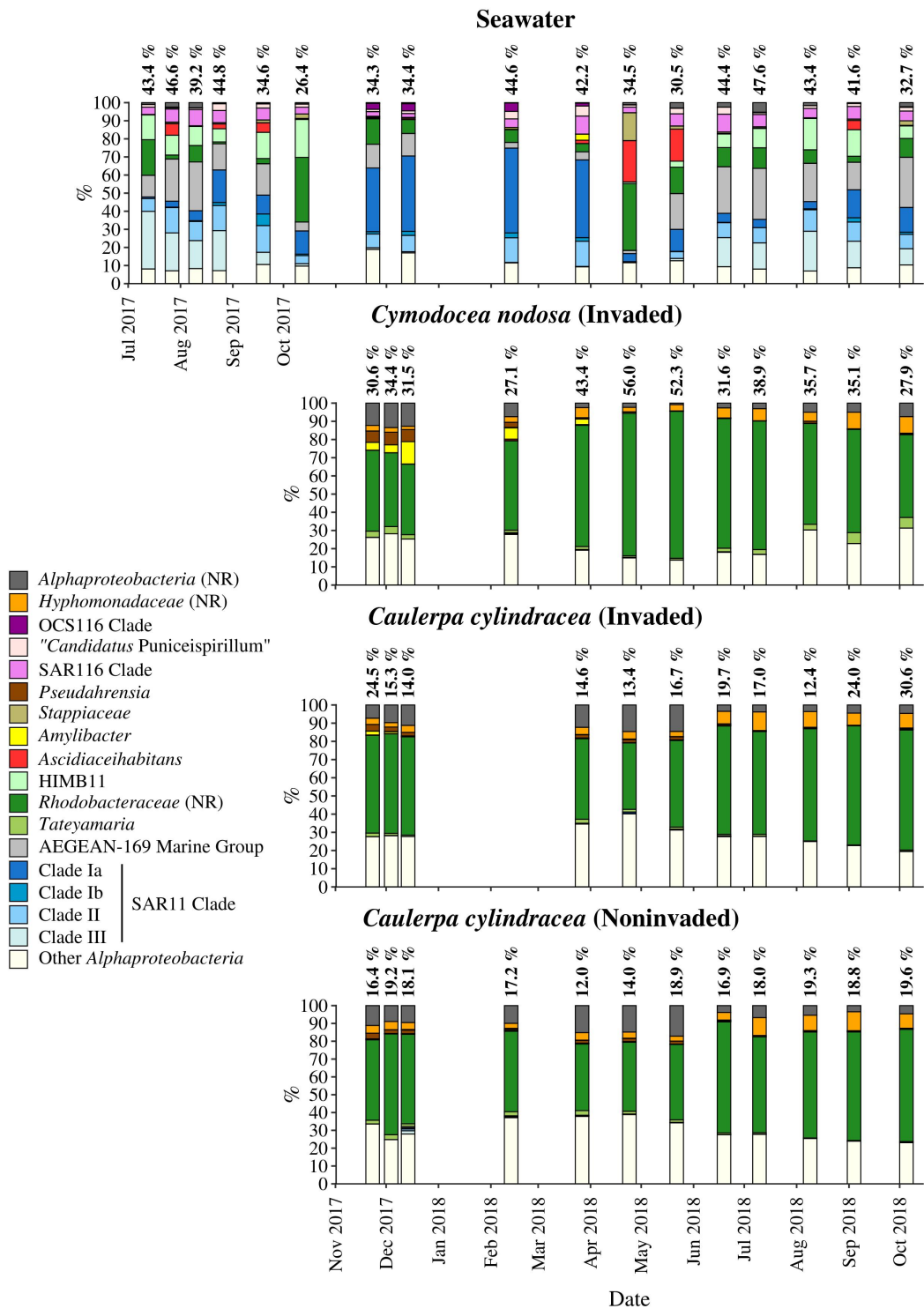


Figure 7. Taxonomic classification and relative contribution of the most abundant alphaproteobacterial sequences on the surfaces of macrophytes (*Cymodocea nodosa* [Invaded] and *Caulerpa cylindracea* [Invaded and Noninvaded]) and in the surrounding seawater. The proportion of alphaproteobacterial sequences in the total bacterial and archaeal community is given above the corresponding bar. NR – No Relative

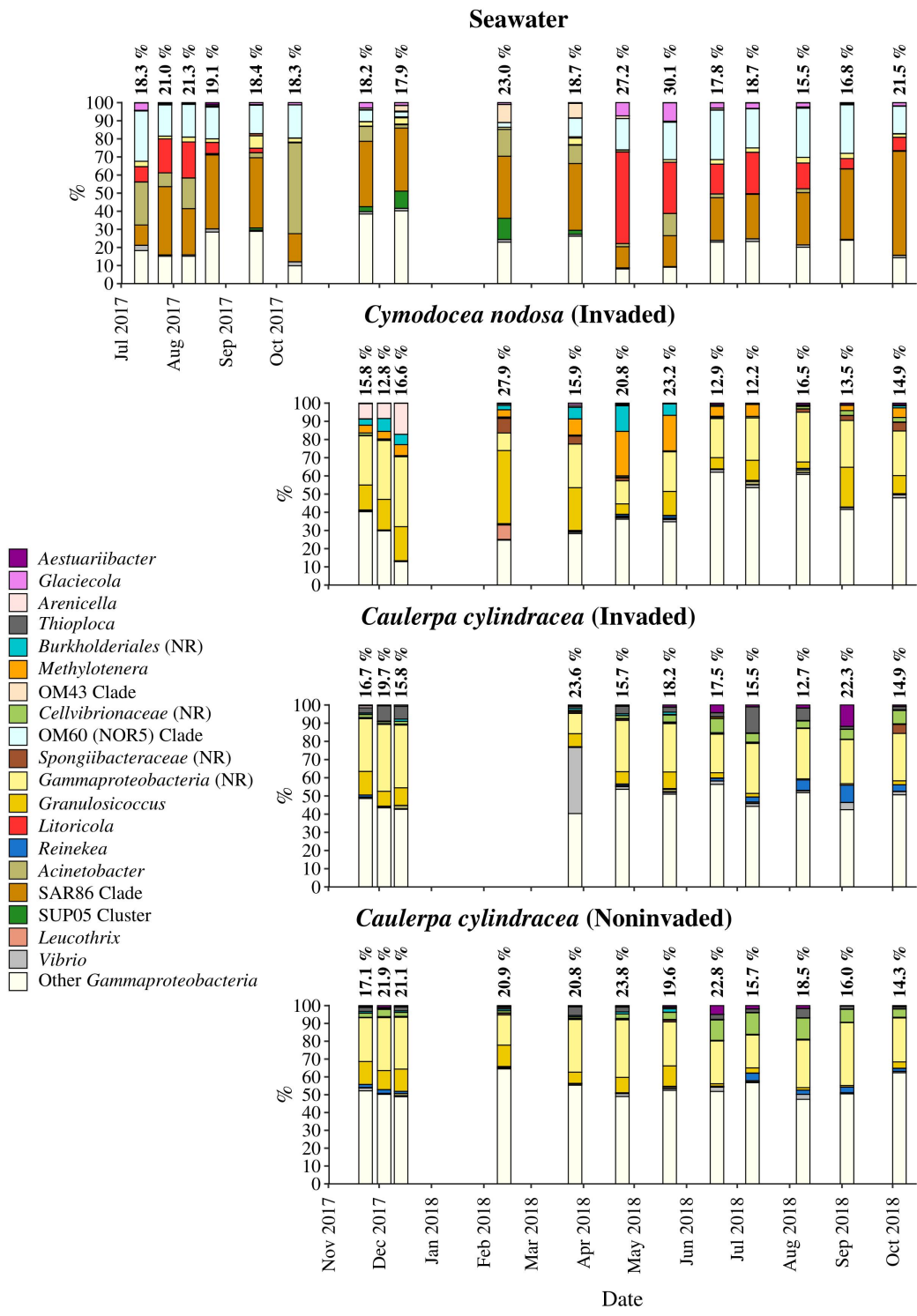


Figure 8. Taxonomic classification and relative contribution of the most abundant gammaproteobacterial sequences on the surfaces of macrophytes (*Cymodocea nodosa* [Invaded] and *Caulerpa cylindracea* [Invaded and Noninvaded]) and in the surrounding seawater. The proportion of gammaproteobacterial sequences in the total bacterial and archaeal community is given above the corresponding bar. NR – No Relative

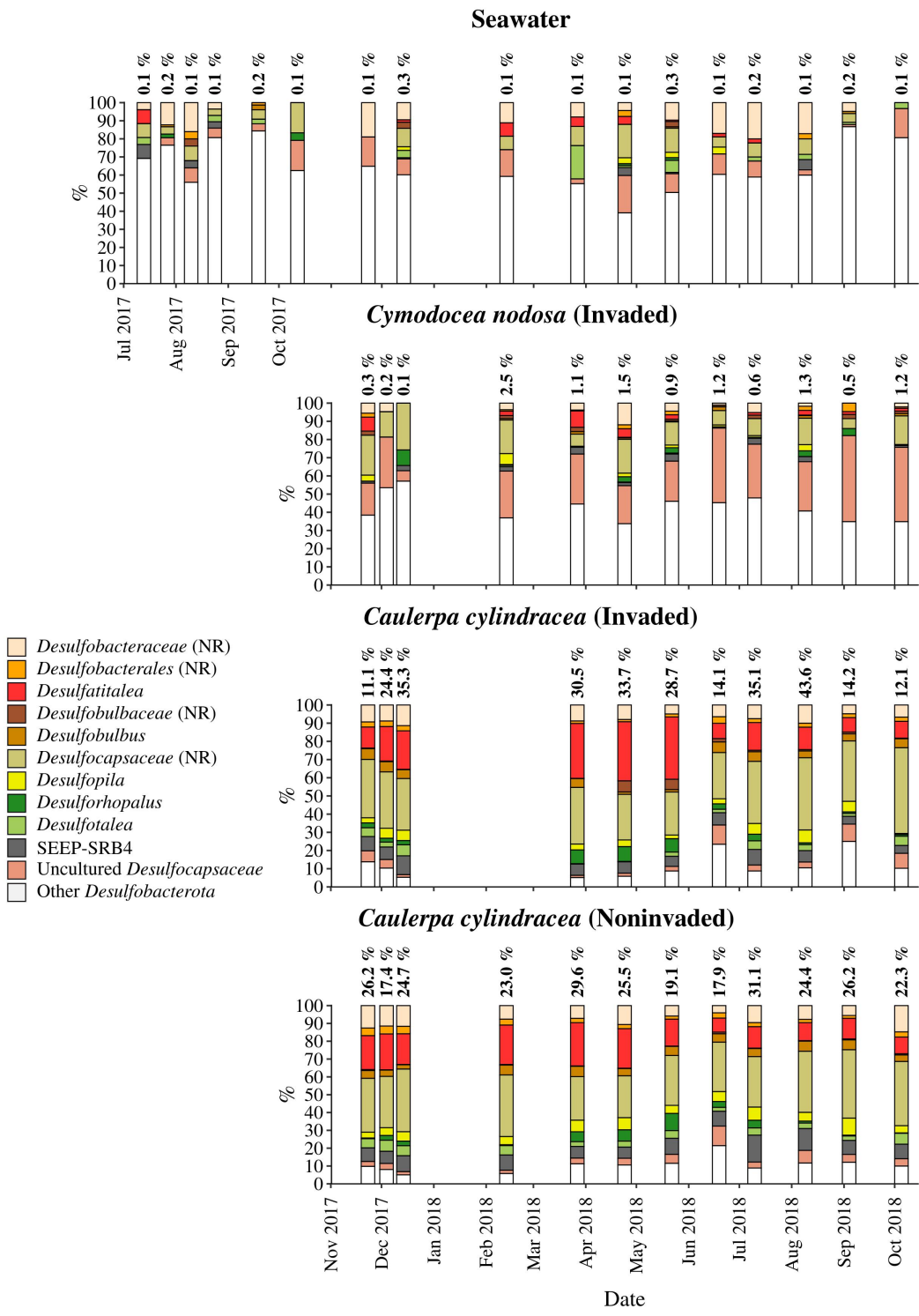


Figure 9. Taxonomic classification and relative contribution of the most abundant sequences within the *Desulfobacterota* on the surfaces of macrophytes (*Cymodocea nodosa* [Invaded] and *Caulerpa cylindracea* [Invaded and Noninvaded]) and in the surrounding seawater. The proportion of sequences classified as *Desulfobacterota* in the total bacterial and archaeal community is given above the corresponding bar. NR – No Relative